Journal of Renewable Materials

Tech Science Press

DOI: 10.32604/jrm.2021.014005

ARTICLE

Removal of Cu(II), Pb(II), Mg(II), and Fe(II) by Adsorption onto Alginate/Nanocellulose Beads as Bio-Sorbent

Ragab E. Abou-Zeid[1], Korany A. Ali[2], Ramadan M. A. Gawad[2], Kholod H. Kamal[3], Samir Kamel[1] and Ramzi Khiari[4,5,6,*]

[1]Cellulose and Paper Department, National Research Centre, Giza, 12622, Egypt

[2]Applied Organic Chemistry Department, Center of Excellence for Advanced Science, National Research Centre, Giza, 12622, Egypt

[3]Water Pollution Research Department National Research Centre, Giza, 12622, Egypt

[4]Faculty of Sciences of Monastir, Research Unit of Applied Chemistry and Environment, University of Monastir, Monastir, 5019, Tunisia

[5]Higher Institute of Technological Studies (ISET) of Ksar-Hellal, Ksar-Hellal, 5070, Tunisia

[6]University of Grenoble Alpes, CNRS, Grenoble INP, LGP2, Grenoble, F-38000, France

[*]Corresponding Author: Ramzi Khiari. Email: khiari_ramzi2000@yahoo.fr

Received: 28 August 2020 Accepted: 29 October 2020

ABSTRACT

Alginate blended with cellulose nanocrystals (CNC), cellulose nanofibers (CNF), and tri-carboxylate cellulose nanofibers (TPC-CNF) prepared and encapsulated in the form of microcapsules (bio-polymeric beads). The cellulosic nanomaterials that used in this study were investigated as nanomaterials for wastewater treatment applications. Batch experiments were performed to study the removal of copper, lead, magnesium, and iron from aqueous solutions by the prepared beads. The effects of the sorbent dosage and the modified polymers on the removing efficiency of the metal cations were examined. Atomic absorption was used to measure the metal ions concentrations. The modified bio-polymeric beads (Alg-CNF, Alg-CNC, and Alg-TPC-CNF) exhibited high-efficiency towards removing of the metal cations; Cu^{2+}, Pb^{2+}, Mg^{2+}, and Fe^{2+}. The Alg-TPC-CNF composite was exhibited excellent removing efficiency which around 95% for Pb, 92% for Cu, 43% for Fe and 54% for Mg. These outcomes affirm that the utilization of nanomaterials giving higher adsorption capacities contrasted with similar material in its micro or macrostructure form.

KEYWORDS

Biopolymers; nanocellulose; alginate; heavy metal removal; wastewater treatment

1 Introduction

Recently, the biopolymers have attracted great attention due to several important features that include natural occurrence, sustainability, low hazards impact on the environment in addition to their economic value [1,2]. Alginate is a linear carboxylate polysaccharide, that extracts from seaweeds, has very high hydrophilicity due to the presence of both carboxylic and hydroxyl groups (Fig. 1). These will increase the tendency towards removing the metal cations from solutions [3]. The cellulosic materials are the most abundant renewable biopolymers in nature and available at low cost for different applications [4,5].

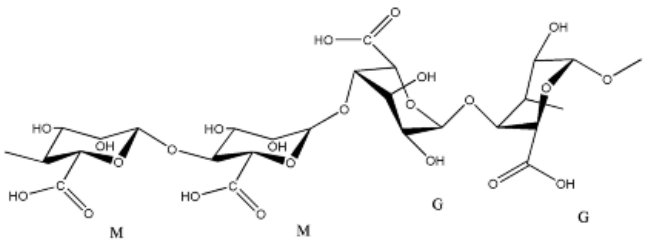

Figure 1: Structure of alginate (Alginate block types: G = guluronic acid, M = mannuronic acid)

The adsorption capacity of the native cellulose towards divalent cations has reported as low adsorption capacity with poor physical stability [6–9]. Thus, many applications were applied to the modified cellulose to achieve an efficient removal tendency for sorption applications [9]. Various applications were applied for the preparation of cellulose nanocomposites from agriculture wastes for environmental applications [10,11]. Currently, the uses of nanocellulose for this subject consists of significant investigation and new possible uses that appear from this study. A large number of studies have devoted to the investigation of cellulose nanomaterials as a promising substrate for waste treatment [12–14]. This due to the unique properties of nanocellulose such as, the mechanical properties, high surface area, hydrophilicity, biodegradability and easy of surface modification of nanocellulose. These excellent properties can be motived the researches to continue to explore the nanomaterial for waste treatment. Such trend has potential to reduce costs with high efficiency in pollution prevention as retention materials (new generations of adsorbents). The nanocellulose can be in the shape of cellulose nanocrystals (CNC) or cellulose nanofibers (CNF) [5,15], CNC can be prepared by acid hydrolysis like sulfuric or phosphoric acid. While CNF is prepared mechanically by mechanical disintegration [16–18]. The negatively charged carboxylate groups on the surface of the TEMPO-Oxidized cellulose nanofibers can lead to interaction with positively charged ions [19]. On the other hand, groundwater is a natural source that provides a valuable part of our needs to clean and safe drinking water. The increase in the number of population and human activities in industry and agricultures lead to increasing in the hardiness and pollution of the groundwater and increasing in the concentration levels of metal cations [20,21]. From these facts and in continuation of our interest for modification and applications of biopolymers for environmental as well as industrial applications [3]. A significant portion of heavy metal emissions are human-induced in wastewater. Major industrial sources include surface treatment processes with elements such as Pb, Cu, Mg, and Fe, as well as industrial products that are discharged into waste at the end of their life [22]. To test the ability of several polymeric matrices of modified alginate with nano-cellulosic materials were investigated for their removing efficiency towards metal cations including Mg^{2+} Fe^{2+}, $Pb^{2+}$and Cu^{2+}.

2 Experimental

2.1 Chemicals and Reagents

Bagasse pulp obtained from Quena Company for paper industry-Egypt was used for extract the cellulose. Sodium alginate, 2,2,6,6-tetramethylpiperidinyloxy (TEMPO), $C_2H_6O_2$, NaOCl, NaBr, $NaIO_4$, $NaClO_2$, NaN_3, $CuSO_4$, Pb $(CH_3COO)_2.3H_2O$, $CaCl_2$, $MgCl_2.6H_2O$ and $FeSO_4.7H_2O$ were bought from Sigma-Aldrich (Germany). H_2SO_4, HCl, CH_3COOH, and NaOH were bought from Elnaser for chemical industry-Egypt. The whole of different reagents were in the analytical grade and were utilized without additional treatment.

2.2 Preparation of Alginate Gel Beads

Alginate gel beads were formulated by dissolving 2.5 g sodium alginate in 100 mL distilled water and 0.002 g NaN_3 as an antimicrobial agent. The solution was stirred by a mechanical stirrer until complete dissolution then dropped using on 2% $CaCl_2$ until complete dissolution then extruded through an INOTECH microencapsulator (Inotech, Suisse) in 2% (w/v) $CaCl_2$ solution as a cross linker for 2 h. The microencapsulator device was used to plan uniform gel beads with 2 mm in diameter by dipping the solution of alginate over a spout of 500 μm. A micrometer and optical microscope were used to determine the size of the prepared beads [3].

2.3 Preparation of Cellulose Nanocrystals (CNC)

As reported by several papers, the CNCs were prepared by hydrolysis treatment [11,23,24]. In 200 mL sulfuric acid (65%), 10 g of pure cellulose fibers were dispersed under mechanical stirring for 25 min. The pulp washed and washed several times using centrifuge (10000 rpm) and dialyzed for a weak until neutrality. The suspension of CNC was sonicated for 10 min before used.

2.4 Preparation of TEMPO-Oxidized Cellulose Fibers

As reported by our previous works [25–28], In 400 mL distilled water 3 g of bagasse pulp, was added to a mixture of TEMPO (0.048 g, 0.3 mmol), sodium bromide (0.48 g, 4.8 mmol), and sodium hypochlorite (30 mL). The pH of the mixture was then adjusted to 10 and stirred for 2 h. Finally, the pH was neutralized using HCl (0.1N). The oxidized cellulose was purified by washing and centrifugation several times and dialyzed for one weak.

2.5 Production of T-CNF and TPC-CNF

Abouzeid et al. [26] were prepared TEMPO and tricarboxylic cellulose nanofiber. In brief: to a mixture of T-CNF (12 g) and NaIO4 (46 mmol) at 60°C in a dark place, an excess amount of ethylene glycol was added with stirring for 3 h. The resulting cellulose dialdehyde was filtered off and washed with water. The aldehyde groups were further oxidized to carboxylic groups by treating with a mixture of sodium chlorite ($NaClO_2$) and acetic acid (1 $mol \cdot L^{-1}$) for 48 h at room temperature. The reaction mixture was filtered off and washed several times with water to afford the tricarboxylic acid CNF.

2.6 Modification of Alginate Gel Beads with Cellulose Nanomaterials

Alginate-nano cellulose composites were prepared by dissolving 2 g of sodium alginate in 100 ml distilled water then mixed with cellulose nanomaterials with ration (5:1) with continuous stirring for 3 h at room temperature. The beads of alginate-nanomaterial composites were prepared by dropping the mixtures in a stirred solution of $CaCl_2$ (2%) using Inotech Encapsulator (Inotech, Suisse).

2.7 Characterization of Nanocomposite Prepared

The morphological properties and the crystallinity index of different prepared nanomaterials were examined using Atomic force Microscopy (AFM) as well as Transmission Electron Microscopy (TEM) and X-ray diffraction pattern (XRD), respectively. AFM tests were employed out in a tapping mode by using Dimension Icon Atomic Force Microscope with an OTESPA cantilever. A concentration of 10^{-4}wt.% of sample was used and it was placed on a mica disk and dried at 80°C during 40 min. Nanoscope III software was handled for the estimation of the diameter from the height profiles of AFM height images. At least five measurements section of the sample were scanned and 200 heights were measured for each test. TEM was used also to evaluate the morphological properties. 0.6 μL of each suspension of nanocellulose was loaded onto a 300 mesh carbon coated formvar copper grids using a labnet micropipette. Water in the suspensions on the carbon coated grids was allowed to evaporate. Additional drop of each prepared nanocellulose suspension was added onto their respective grids to

increase the amount of cellulose particles and the process was repeated several times. The nano-samples coated grids were examined using JEOL 200CX transmission electron microscope at 80 kV. The XRD of the prepared samples were recorded at room temperature using X-ray diffractometer (PANalytical-Netherland) with a monochromatic radiation source (Cu-Kα; λ = 0.154 nm), scanning time 5 min, with 2 angles (from 5 to 60°) scan mode. Segal method [29] used for calculation of the crystallinity index of the new samples of this study from the top band of (200) peak ($I_{200}2\theta$ = 22). The minimum intensity between 200 and 110 peaks ($I_{am}2\theta$ = 18), where I_{200} represent the crystalline material and I_{am} represent the amorphous material. The analysis of FTIR spectra were conducted using a Perkin Elmer FT-IR spectrometer (Perkin Elmer, USA). The disks that were used for the analysis were prepared by mixing 10 mg of the tested material with 250 mg of KBr. The range of the wavenumber was from 4000 to 500 cm^{-1} with a resolution of 4 cm^{-1} and an accumulation of 32 scans per analysis.

As reported by several researches that the carboxyl groups' content on CNF and TPC-CNF were established by the conductivity titration technique [26,30]. In brief, 50 mg of oxidized cellulose was mixed into 15 ml of 0.01 mol L^{-1} hydrochloric acid solutions with stirring for 30 min, after that the solution was titrated with 0.01 mol L^{-1} NaOH. The carboxyl content was evaluated according to the Eq. (1):

$$n(\mathrm{COOH}) = (V_b - V_a) \times 0.01 \quad (1)$$

The measurements were established at least in three times. Where V_a corresponding to the excess of HCl and a weak one (V_b) associated with the carboxyl content.

2.8 Nanomaterials for Batch Adsorption

During this section, the efficiency of the prepared nanomaterials for batch adsorption was established. The removing capacity of the prepared bio-polymeric matrixes was evaluated by treatment with the initial concentrations Cu(II) 200 mg L^{-1} and Pb(II) 300 mg L^{-1}, Mg (II) 200 mg L^{-1} and Fe(II) 250 mg L^{-1} salts solutions with the new matrixes. The salts solutions used in this study were prepared by using $CuSO_4$, $Pb(CH_3COO)_2.3H_2O$, $MgCl_2.6H_2O$, and $FeSO_4.7H_2O$ in distilled water. 1 g, 1.5 g and 2 g of Alg 2.5%, Alg–CNP, Alg-CNC, and Alg-CNF beads were added to each the metal solutions with shaking at 200 r/min and 25 ± 2°C for two hours contact time to reach the equilibrium. The adsorption pH was kept at 6.0. Either 0.1 mol/L HCl or 0.1 mol/L NaOH solutions were used to adjust the pH values during the sorption experiments. The final metals concentrations were determined by atomic absorption spectrometer (PerkinElmer 3110, USA). Atomic absorption quantities were established out in an air-acetylene flame. The experimental conditions were done is bellow: Absorption line: 324.75, 217.1, 285.21, and 248.33 nm; slit widths, 0.165, 0.66, 0.7, and 0.7 nm; and lamp currents, 20, 15, 18 and 15 mA for Cu, Pb, Mg, and Fe ions, respectively.

To evaluate the capacity of the new composites to remove the metal cations, the following equation was used to calculate the removing efficiency percentage (R).

$$R = \left(C_o - \frac{C_t}{C_o}\right) \times 100 \quad (2)$$

where, C_o: The initial ions concentration (mg L^{-1}), C_t (mg L^{-1}), the remaining ions concentration after a period of time (t), the measurements were repeated in triplicate

The adsorption performance experiment was performed by mixing of the adsorbent with the adsorbate solution at controlled concentrations. The experiments have been done at neutral pH and room temperature. The adsorption capacity of hydrogel was calculated according the following equation:

$$q_e = \frac{(C_o - C_e)V}{m} \tag{3}$$

where q_e is the amount of pollutant adsorbed ($mg \cdot g^{-1}$), C_o ($mg \cdot L^{-1}$) and C_e ($mg \cdot L^{-1}$) are the initial pollutant solution concentration and the equilibrium concentration of pollutant in the bulk solution. V (L) is the volume of solution, and m (g) is the weight of the adsorbent.

3 Results and Discussions

3.1 Characterizations of the Prepared: CNC, TEMPO-CNF and Tricarboxylic CNF

As described by several reported [31–33], controlled acid hydrolysis treatment was used for the preparation of CNC from the dissolved pulp. This process removes the amorphous region in the cellulose fibers and reduces the size from the microscale to the nanoscale. The structures of the prepared CNC were evaluated by TEM, FT-IR, and XRD analysis, and the result was regrouped in Fig. 2. From this Fig. 2A, it can be concluded that the TEM pattern of the newly prepared CNC confirms well the success of the preparation. In fact, the CNC dimensions were evaluated using a digital image, obtained by TEM, analysis (Image J) as an average of 90 individual measurements, revealed that the length and of the width was in the range of 80–180 nm and of 4–8 nm, respectively. Such results are in accordance with our previously published paper [11,34,35].

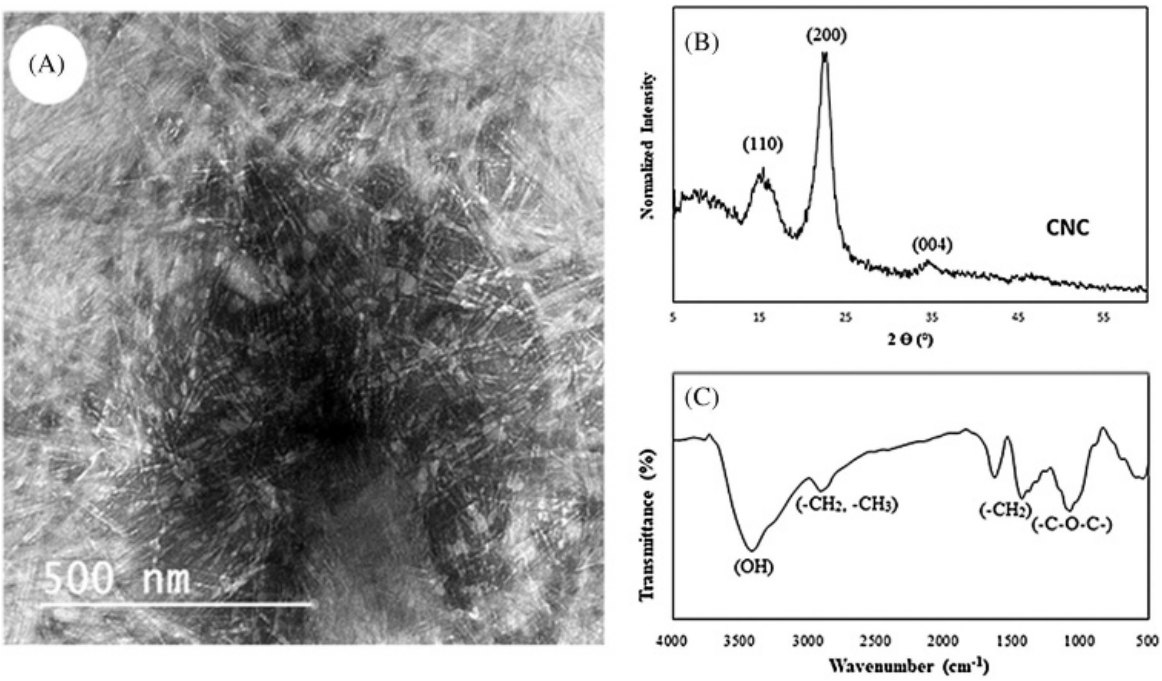

Figure 2: TEM (A), XRD (B) and FT-IR (C) of the prepared newly prepared CNC. Adapted with permission [3]. Copyright© 2018, Springer

The XRD pattern (Fig. 2B) revealed the known peaks of the cellulose I with crystalline peaks at 2θ =15.4°, 22.3°, and 34.6°. The later peaks compatible with the typical structure of cellulose I with planes (110), (200), and (004) respectively. The crystallinity index of CNC was calculated and equal to 0.85. This explains the increasing crystalline part increased than the amorphous part of cellulose fiber during hydrolysis. The FT-IR spectrum of the prepared CNC (Fig. 2C) showed a typical structure of cellulose where were characterized by a dominant OH stretch band (3400–3424 cm^{-1}) and a CH stretch

band (2896–2925 cm^{-1}) conforming to the aliphatic moieties in polysaccharides. The absorption band at 1118 cm^{-1} was assigned to COH skeletal vibration. The COC pyranose ring skeletal vibration gave a prominent band at 1048 cm^{-1}. A slight band detected at 900 cm^{-1} represent the glycosidic deformation with ring vibration contribution and OH bending, which is characteristic of the glycosidic linkages between glucose units in cellulose. The characterization of (T-CNF) and (TPC-CNF) which was carried out by using the TEM, XRD, and FT-IR analysis. The obtained results were recapitulated in Figs. 3–5 and confirm that TEMPO-oxidation followed by periodate-chlorite oxidation were applied on the dissolved bagasse pulp fibers to achieve successful Nano fibrillate. Fig. 3 displays the AFM images of the T-CNF and TPC-CNF dispersions with various carboxyl contents from 0.8 to 2.3 m·mol g^{-1} which displays the successfully nano-fibrillated of TEMPO-oxidized pulp. The increase in the carboxyl content from 0.8 to 2.3 mmol g^{-1} leads to the nanofibers becoming finer in width. This is due to a releasing bonding of fibers with increasing the repulsions between surface charges.

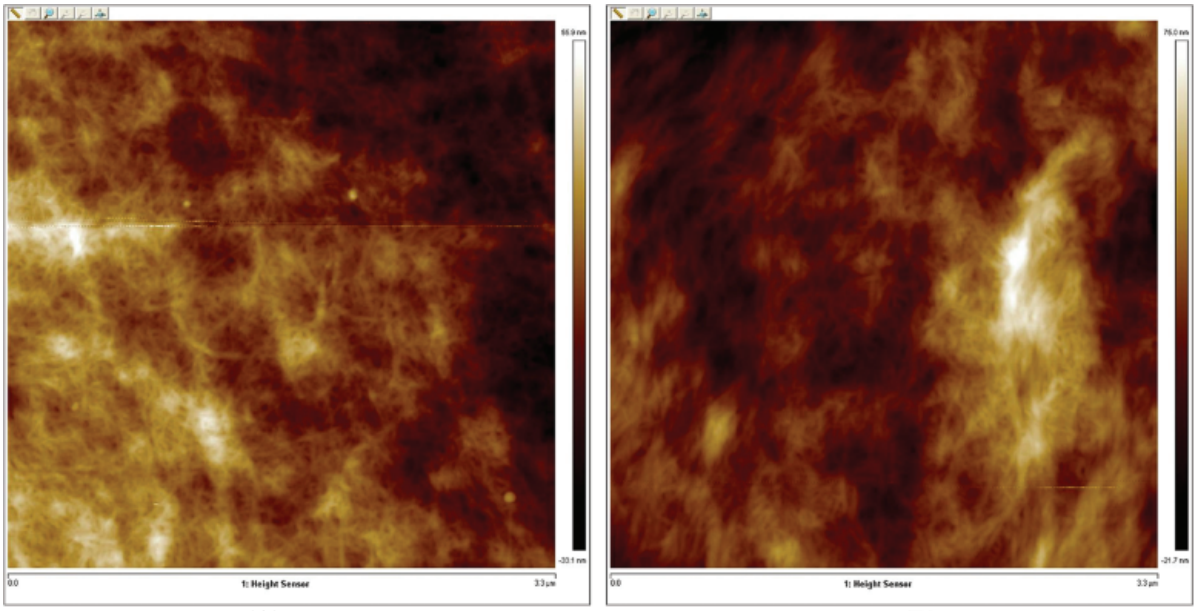

Figure 3: AFM of T-CNF (A), and TPC-CNF (B)

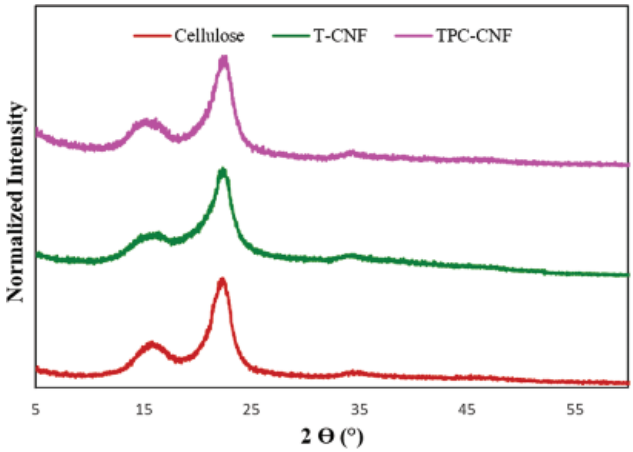

Figure 4: XRD diffraction patterns TC-CNF and TPC-CNF

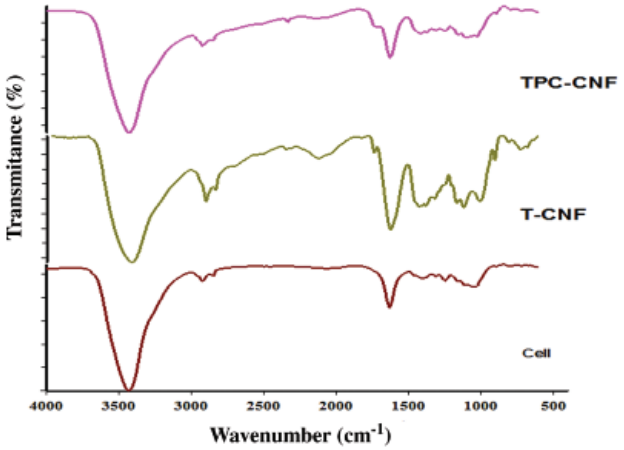

Figure 5: FTIR spectra of cellulose fibers, T-CNF and TPC-CNF

The X-ray diffraction of the prepared samples as illustrated in Fig. 4 and the effect of oxidation on the crystallinity were studied. The X-ray pattern confirms again a cellulose type 1 was observed with characteristics peaks at 2θ at 16°, 22.5°, and 34°, which correspond to the (110), (200), and (004) crystallographic planes, respectively.

Fig. 5 summarized the FT-IR curves of cellulose, TC-CNF and TPC-CNF revealed wide peaks at 3360 cm^{-1} for the stretching vibration of -OH groups. The bands observed at 1298 cm^{-1} are corresponding to bending vibration of OH. Other bands have appeared at 2900 cm^{-1}, 1416 cm^{-1} and 1015 cm^{-1} related which attributed to the CH, -CH_2, and CH_2-O-CH_2 groups respectively. The carbonyl of the carboxylic group of TC-CNF and TPC-CNF that confirms the oxidation process has appeared at 1740 cm^{-1}. This band confirms again the well successful of TC-CNF and TPC-CNF preparations.

3.2 Characterization of Bio Nano Sorbent for Removing Metal Cations Capacity

Three matrixes of alginate-nano-cellulose composites were prepared namely: Alginate/CNC, alginate/TC-CNF, and alginate/TPC-CNF. The alginate and the modified alginate were prepared in the form of beads with a diameter of 2 mm using the INOTECH microencapsulator (Inotech, Suisse). These samples were used in order to increase the alginate selectivity toward removing of the Cu, Pb, Mg, and Fe metal cations from water as taking as an example for this present study.

The scanning electron microscope (SEM) of the prepared beads (Fig. 6) was used to show the overall shapes and the surface morphologies of prepared beads. The overall shape of the beads was spherical with a somewhat rough surface appearance. Also, from the SEM images, it was observed a difference in appearance between the prepared beads. This modification can be attributed to the difference between the uses of cellulose nanomaterials. The alginate/CNC beads had relatively smooth surfaces, while alginate/T-CNF and alginate/TPC-CNF beads showed a more granular structure. This result shows the good homogeneity of cellulose nanocrystals with alginate.

3.3 Macroscopic Adsorption Data: Sorption Study

The prepared alginate beads and their nanocomposites were tested for efficient removal of the metal cations from aqueous solutions. The alginate scaffolds can provide several sites to coordinate with several metal cations via coordination interaction of the metal cations and their functional group (free carboxyl groups). The removal of metal ions (Cu^{2+}, Pb^{2+}, Mg^{2+}, and Fe^{2+}) from the prepared solutions by alginate and their nanocomposites (Alg, Alg-CNC, Alg-TC-CNF, and Alg-TPC-CNF) were studied by varying the

adsorbents dosages from 1 to 2 g while keeping the conditions such as pH, contact time, temperature and initial metal ion concentration constant.

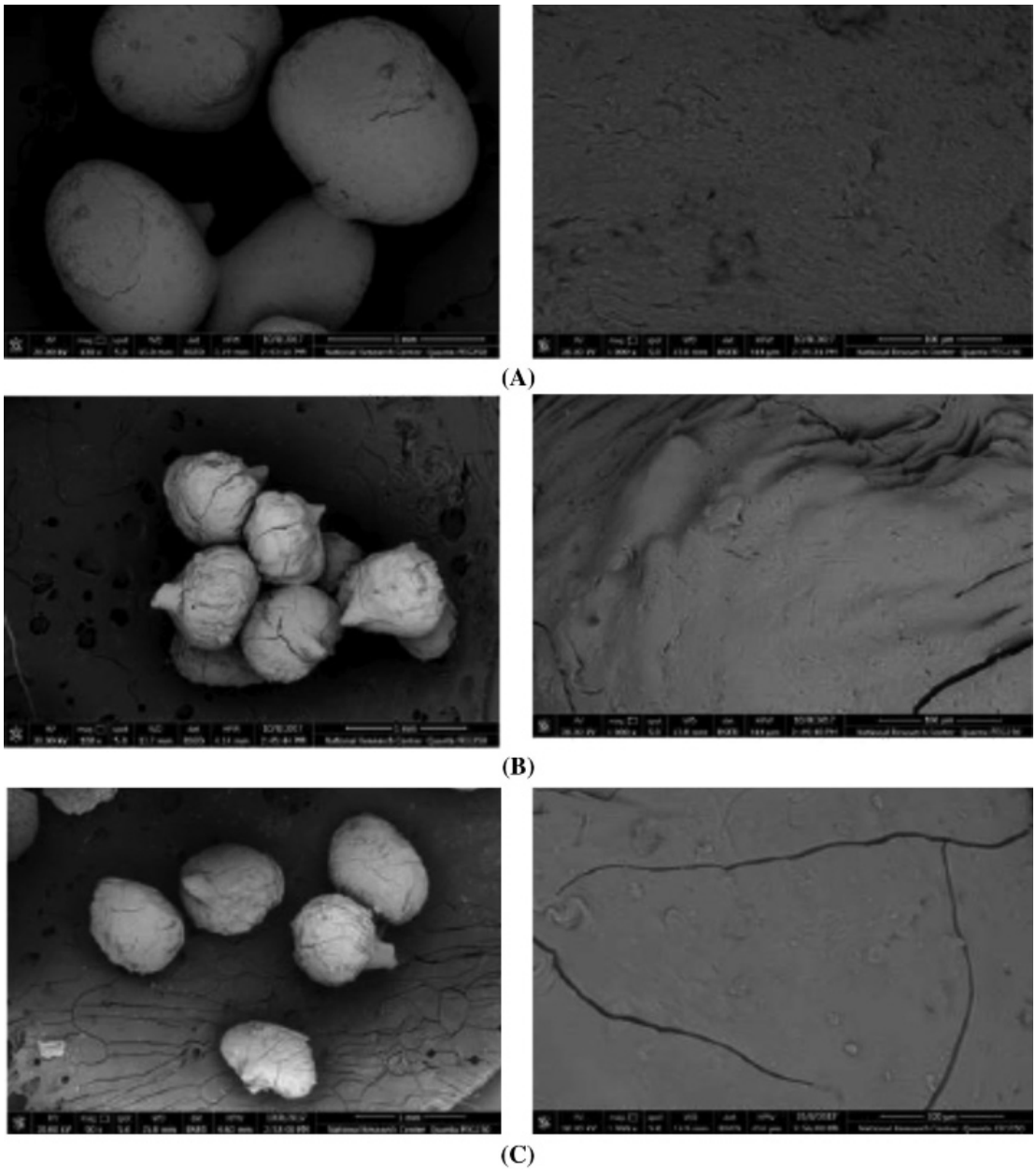

Figure 6: SEM images of (A) Alg/CNC beads, (B) Alg /T-CNF and (C) Alg/TPC-CNF beads

Fig. 7 shows the effect of the sorbent dosage on the removal efficiency of Cu^{2+}, Pb^{2+}, Mg^{2+}, and Fe^{2+}ions. It was observed the metals removal increases with rising the dose of alginate and their nanocomposites. That could be a result the number of anionic groups on the surface of the beads [3,36]. From this figure, it can be also illustrated that the ability of the alginate polymeric matrix concerning the elimination of the cationic heavy metals almost increase with the modified cellulosic materials; Alg-CNC, Alg-CNF, and Alg-TPC-CNF, respectively. The Alg-TPC-CNF has the maximum removal efficiency than

the rest of nanocomposites due to its higher carboxylate content (2 mmol g^{-1}). It is clear that the increased number of carboxylic groups increase the efficiency of heavy metal removal [3].

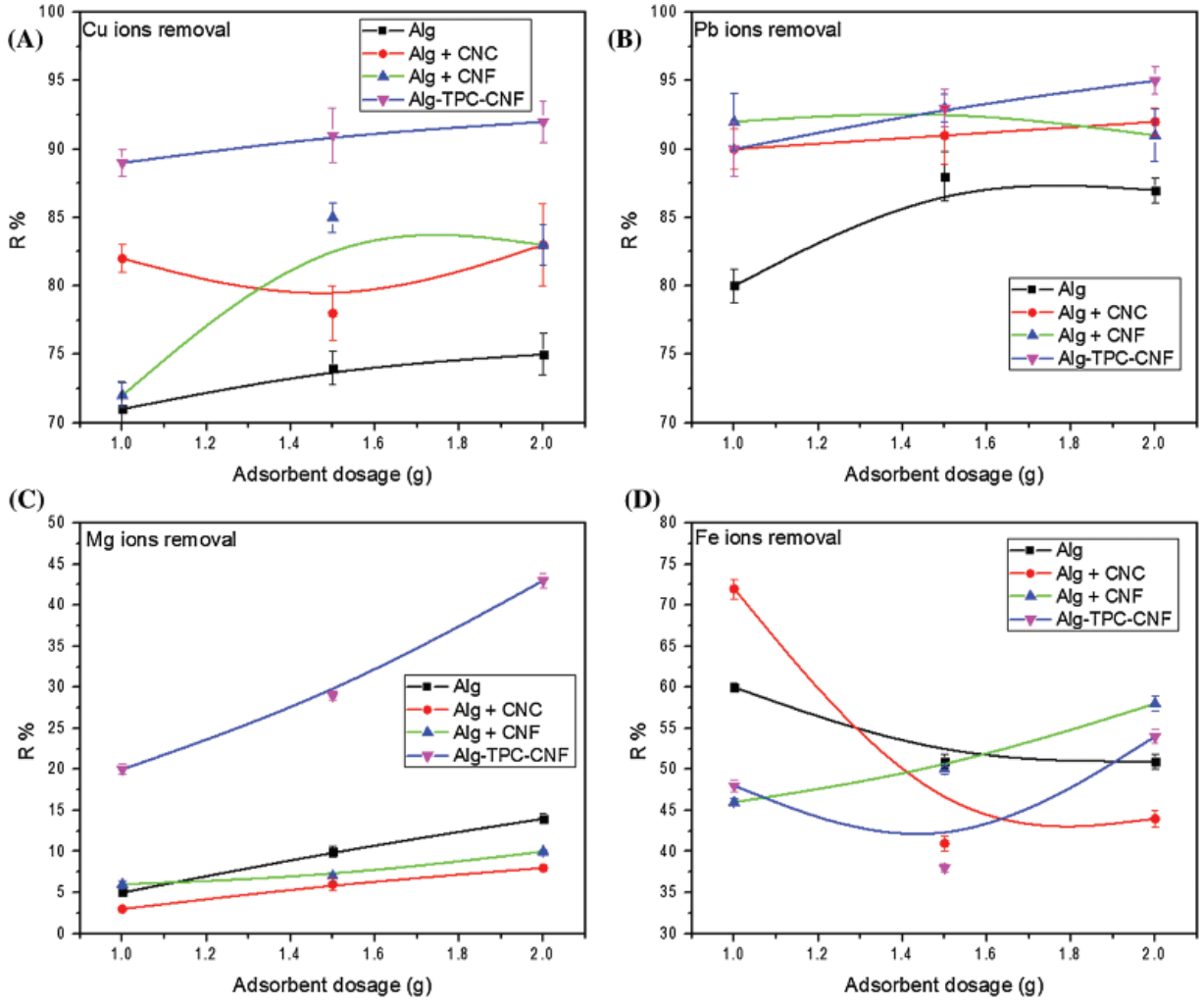

Figure 7: Effect of sorbents dosage on the removal efficiency of (A) $Pb^{2+,}$ (B) Cu^{2+}, (C) Mg^{2+} and (D) Fe^{2+}

Despite the group alkaline earth metals is more reactive than the group of metal transition (Fe, Cu and Pb), it can be explain by the effect of electronegativity where when the proton number is higher, the electronegativity have the same trend. In addition, the surface group plays a significant parameter in the adsorption capacity. Since, the total charge affect directly the uptake capacity.

A comparison between our prepared nanomaterials with the various adsorbents [37–41] was documented in Tab. 1. It can be concluded from this table as well as the previously figure that the presence of sulfate groups on the CNC as a result of its extraction process using a sulfuric acid hydrolysis step can increase the adsorption capacity of cationic species. Thus, the adsorption capacity of Mg^{2+} for CNC and CNF were 68.4 mg g^{-1} and 61.7 mg g^{-1} respectively. This increase in adsorption capacity of CNC is due to the sulfate groups with the same applies for the others adsorption ions metals. The nanomaterials were employed to eliminate Fe^{2+} from aqueous solution. It was noticed that the rate of adsorption was very quickly, in particularly for all prepared samples. It was observed that a complexation

process can be making between the heavy metals adsorption with the prepared samples. While the main mechanism for removing of heavy metal ions using the prepared nanocomposites materials was established by ion-exchange. Due to the ion-exchange mechanism, the nanocomposites materials revealed a large adsorption capacity for Fe^{2+} (230 mg g^{-1}).

Table 1: The heavy metal ions adsorption capacities of alginate and/or cellulose nanomaterials

Adsorbate	Adsorbent	pH	q_e (mg g^{-1})	Reference
Mg^{2+}	Alg	6–7	83.3	This work
	Alg + CNC	6–7	68.4	This work
	Alg + CNF	6–7	61.7	This work
	Alg + TPC-CNF	6–7	82.9	This work
Cu^{2+}	Alg	6–7	47.8	This work
	Alg + CNC	6–7	53.4	This work
	Alg + CNF	6–7	41.4	This work
	Alg + TPC-CNF	6–7	62.4	This work
	CNC/Sulfate ($-SO_3^-$)	4.5	17.9	[37]
		6.2	112	[38]
	CNF/Tempo	6	49.0	[38]
Pb^{2+}	Alg	6–7	52.0	This work
	Alg + CNC	6–7	76.8	This work
	Alg + CNF	6–7	79.8	This work
	Alg + TPC-CNF	6–7	68.2	This work
	CNC/Sulfate ($-SO_3^-$)	5.5	47.0	[39]
	Carboxylated CNC/alginate composite	5.2	280	[40]
Fe^{2+}	Alg	6–7	212.5	This work
	Alg + CNC	6–7	234.8	This work
	Alg + CNF	6–7	227.5	This work
	Alg + TPC-CNF	6–7	230.3	This work
Fe^{3+}	CNC/Sulfate ($-SO_3^-$)	3.5–4.5	6.3	[41]
	CNF/Phosphorylation ($-PO_3^{2-}$)	3.5–4.5	73.0	[41]

The overall conclusion to be deduced from this part is that even with the difference in the heavy metal ions adsorption by the prepared materials, the cellulose nanomaterials display the notable resources of cellulose, for example, low density, low cost, renewability, sustainability, biodegradability, abundance and availability in a variety of forms, non-toxicity/biocompatibility, and probability to create energy without residue after burning at the end of their life-cycle can be used as promising efficient adsorbent and adaptable membrane included in the preparation of hybrid materials for wastewater treatment. However, isolation of cellulose nanomaterials is the step also important because it can be generating many groups and/or charges which affect consequently into adsorption capacity. That is why this work open a new window to continue study the lower and higher dosages of adsorbents as well as to use both macroscopic

and microscopic data to understand the adsorption mechanism. This relevance of this work will be reported very soon.

4 Conclusions

This investigation highlights the activity of alginate and blended alginate with cellulosic nanomaterials towards removing the divalent cations; Cu^{2+}, Pb^{2+}, Mg^{2+}, and Fe^{2+} from their aqueous solution. These materials present many advantages comparing the useful product: Bioresources, low cost, natural products, etc. Remarkably, the metal ion removal efficiency approximately increases with the increase in the absorbent dose. The Alg-CNF-TPC almost has the maximum removing efficiency rather than the rest of nanocomposites due to its higher carboxylate content.

Funding Statement: The authors acknowledge the Science and Technology Development Fund (STDF), Egypt for financial support of the research activities related to the project; Project ID 15203. The authors also gratefully express their sincere gratitude to the "PHC-UTIQUE CMCU" (18G1132) and the CMPTM (17TM22), as well as to the Tunisian Ministry of Higher Education for the financial support. Ramzi KHIARI received the "Young Researcher Encouragement Prize 2020, from the Tunisian Academy of Sciences, Letters and Arts Beit al-Hikma, Tunisia.

Conflicts of Interest: The authors declare that they have no conflicts of interest to report regarding the present study.

References

1. Samir, K., Hussein, A. Y., El-Sakhawy, M. (2004). Copper(II) ions adsorption onto cationic oxycellulose. *Energy Education Science and Technology, 14,* 51–60.
2. K. Hussein, A. Y., El-Sakhawy, M. (2004). Copper(II) ions adsorption onto cationic oxycellulose. *Energy Education Science and Technology, 14(2),* 51–60.
3. Ali, K. A., Wahba, M. I., Abou-zeid, R., Kamel, S. (2019). Development of carrageenan modified with nanocellulose-based materials in removing of Cu^{2+}, Pb^{2+}, Ca^{2+}, Mg2+, and Fe^{2+}. *International Journal of Environmental Science and Technology, 16(10),* 5569–5576. DOI 10.1007/s13762-018-1936-z.
4. Kamel, S., Abou-Yousef, H., Yousef, M., El-Sakhawy, M. (2012). Potential use of bagasse and modified bagasse for removing of iron and phenol from water. *Carbohydrate Polymers, 88(1),* 250–256. DOI 10.1016/j.carbpol.2011.11.090.
5. Klemm, D., Kramer, F., Moritz, S., Lindström, T., Ankerfors, M. et al. (2011). Nanocelluloses: A new family of nature-based materials. *Angewandte Chemie-International Edition, 50(24),* 5438–5466. DOI 10.1002/anie.201001273.
6. Moon, R. J., Martini, A., Nairn, J., Simonsen, J., Youngblood, J. (2011). Cellulose nanomaterials review: Structure, properties and nanocomposites. *Chemical Society Reviews, 40(7),* 3941–3994. DOI 10.1039/c0cs00108b.
7. El Khames Saad, M., Khiari, R., Elaloui, E., Moussaoui, Y. (2014). Adsorption of anthracene using activated carbon and Posidonia oceanica. *Arabian Journal of Chemistry, 7(1),* 109–113. DOI 10.1016/j.arabjc.2013.11.002.
8. Khiari, R., Dridi-Dhaouadi, S., Aguir, C., Mhenni, M. F. (2010). Experimental evaluation of eco-friendly flocculants prepared from date palm rachis. *Journal of Environmental Sciences, 22(10),* 1539–1543. DOI 10.1016/S1001-0742(09)60286-2.
9. Abou-Zeid, R. E., Khiari, R., El-Wakil, N., Dufresne, A. (2019). Current state and new trends in the use of cellulose nanomaterials for wastewater treatment. *Biomacromolecules, 20(2),* 573–597. DOI 10.1021/acs.biomac.8b00839.
10. Abouzeid, R. E., Khiari, R., Beneventi, D., Dufresne, A. (2018). Biomimetic mineralization of three-dimensional printed alginate/tempo-oxidized cellulose nanofibril scaffolds for bone tissue engineering. *Biomacromolecules, 19 (11),* 4442–4452. DOI 10.1021/acs.biomac.8b01325.

11. Abou-Zeid, R. E., Hassan, E. A., Bettaieb, F., Khiari, R., Hassan, M. (2015). Use of cellulose and oxidized cellulose nanocrystals from olive stones in chitosan bionanocomposites. *Journal of Nanomaterials, 16(8),* 1–11. DOI 10.1155/2015/687490.
12. Liu, P., Sehaqui, H., Tingaut, P., Wichser, A., Oksman, K. et al. (2014). Cellulose and chitin nanomaterials for capturing silver ions (Ag+) from water via surface adsorption. *Cellulose, 21(1),* 449–461. DOI 10.1007/s10570-013-0139-5.
13. Sehaqui, H., De Larraya, U. P., Liu, P., Pfenninger, N., Mathew, A. P. et al. (2014). Enhancing adsorption of heavy metal ions onto biobased nanofibers from waste pulp residues for application in wastewater treatment. *Cellulose, 21(4),* 2831–2844. DOI 10.1007/s10570-014-0310-7.
14. Kardam, A., Raj, K. R., Srivastava, S., Srivastava, M. M. (2014). Nanocellulose fibers for biosorption of cadmium, nickel, and lead ions from aqueous solution. *Clean Technologies and Environmental Policy, 16(2),* 385–393. DOI 10.1007/s10098-013-0634-2.
15. Rahimi Kord Sofla, M., Brown, R. J., Tsuzuki, T., Rainey, T. J. (2016). A comparison of cellulose nanocrystals and cellulose nanofibres extracted from bagasse using acid and ball milling methods. *Advances in Natural Sciences: Nanoscience and Nanotechnology, 7(3),* 035004. DOI 10.1088/2043-6262/7/3/035004.
16. Tahiri, C., Vignon, M. R. (2000). TEMPO-oxidation of cellulose: Synthesis and characterisation of polyglucuronans. *Cellulose, 7(2),* 177–188. DOI 10.1023/A:1009276009711.
17. Tang, Z., Li, W., Lin, X., Xiao, H., Miao, Q. et al. (2017). TEMPO-Oxidized cellulose with high degree of oxidation. *Polymers, 9(12),* 421–431. DOI 10.3390/polym9090421.
18. El-Gendy, A., Abou-Zeid, R. E., Salama, A., Diab, M., El-Sakhawy, M. (2017). TEMPO-oxidized cellulose nanofibers/polylactic acid/TiO_2 as antibacterial bionanocomposite for active packaging. *Egyptian Journal of Chemistry, 60(6),* 4–8. DOI 10.21608/ejchem.2017.1835.1153.
19. Isogai, A., Saito, T., Fukuzumi, H. (2011). TEMPO-oxidized cellulose nanofibers. *Nanoscale, 3(1),* 71–85. DOI 10.1039/C0NR00583E.
20. Carpenter, A. W., De Lannoy, C. F., Wiesner, M. R. (2015). Cellulose nanomaterials in water treatment technologies. *Environmental Science & Technology, 49(9),* 5277–5287. DOI 10.1021/es506351r.
21. Masindi, V., Muedi, K. L. (2018). Environmental contamination by heavy metals. *Heavy Metals. Intechopen*. DOI 10.5772/intechopen.76082.
22. Baysal, A., Ozbek, N., Akm, S. (2013). Determination of trace metals in waste water and their removal processes. *Waste water—Treatment technologies and recent analytical developments*. INTECH Europe.
23. Bettaieb, F., Khiari, R., Dufresne, A., Mhenni, M. F., Belgacem, M. N. (2015). Mechanical and thermal properties of Posidonia oceanica cellulose nanocrystal reinforced polymer. *Carbohydrate Polymers, 123,* 99–104. DOI 10.1016/j.carbpol.2015.01.026.
24. Khiari, R., Belgacem, M. N. (2017). Potential for using multiscale Posidonia oceanica waste: Current status and prospects in material science. *Lignocellulosic fibre and biomass-based composite materials.* Processing, Properties and Applications Woodhead Publishing Series in Composites Science and Engineering, pp. 447–471. Elsevier, DOI 10.1016/B978-0-08-100959-8.00021-4.
25. Khiari, R. (2017). Valorization of agricultural residues for cellulose nanofibrils production and their use in nanocomposite manufacturing. *International Journal of Polymer Science, 2017(9),* 1–10. DOI 10.1155/2017/6361245.
26. Abou-Zeid, R. E., Dacrory, S., Ali, K. A., Kamel, S. (2018). Novel method of preparation of tricarboxylic cellulose nanofiber for efficient removal of heavy metal ions from aqueous solution. *International Journal of Biological Macromolecules, 119,* 207–214.
27. Hassan, E., Hassan, M., Abou-zeid, R., Berglund, L., Oksman, K. et al. (2017). Use of bacterial cellulose and crosslinked cellulose nanofibers membranes for removal of oil from oil-in-water emulsions. *Polymers, 9(9),* 388–402.
28. Hassan, M. L., Fadel, S. M., Abouzeid, R. E., Elseoud, W. S. A. (2020). Water purification ultrafiltration membranes using nanofibers from unbleached and bleached rice straw. *Scientific Reports, 10,* 1–9. DOI 10.1038/s41598-020-67909-3.

29. Segal, L., Creely, J. J., Martin, A. E., Conrad, C. M. (1959). An empirical method for estimating the degree of crystallinity of native cellulose using the X-ray diffractometer. *Textile Research Journal, 29,* 786–794.
30. Da Silva Perez, D., Montanari, S., Vignon, M. R. (2003). TEMPO-mediated oxidation of cellulose III. *Biomacromolecules, 8(8),* 2485–2491.
31. Bondeson, D., Mathew, A., Oksman, K. (2006). Optimization of the isolation of nanocrystals from microcrystalline cellulose by acid hydrolysis. *Cellulose, 13,* 171–180.
32. Johar, N., Ahmad, I., Dufresne, A. (2012). Extraction, preparation and characterization of cellulose fibres and nanocrystals from rice husk. *Industrial Crops and Products, 37,* 93–99.
33. Siqueira, G., Tapin-Lingua, S., Bras, J., da Silva Perez, D., Dufresne, A. (2011). Mechanical properties of natural rubber nanocomposites reinforced with cellulosic nanoparticles obtained from combined mechanical shearing, and enzymatic and acid hydrolysis of sisal fibers. *Cellulose, 18,* 57–65.
34. Alothman, O. Y., Kian, L. K., Saba, N., Jawaid, M., Khiari, R. (2021). Cellulose nanocrystal extracted from date palm fibre: Morphological, structural and thermal properties. *Industrial Crops and Products, 159(113075),* 1–7.
35. Hassan, M. L., Abou-Zeid, R. E., Fadel, S. M., El-Sakhawy, M., Khiari, R. (2014). Cellulose nanocrystals and carboxymethyl cellulose from olive stones and their use to improve paper sheets properties. *International Journal of Nanoparticles, 7,* 261–277.
36. Aziz, F., Achaby, M. E., Lissaneddine, A., Aziz, K., Ouazzani, N. et al. (2019). Composites with alginate beads: A novel design of nano-adsorbents impregnation for large-scale continuous flow wastewater treatment pilots. *Saudi Journal of Biological Sciences, 10,* 2499–2508.
37. Zhang, X., Zhao, J., Cheng, L., Lu, C., Wang, Y. et al. (2014). Acrylic acid grafted and acrylic acid/sodium humate grafted bamboo cellulose nanofibers for cu^{2+} adsorption. *RSC Advances, 4,* 55195–55201.
38. Sehaqui, H., Perez De Larraya, U., Liu, P., Pfenninger, N., Mathew, A. P. et al. (2014). Enhancing adsorption of heavy metal ions onto biobased nanofibers from waste pulp residues for application in wastewater treatment. *Cellulose, 21,* 2831–2844.
39. Yu, X., Tong, S., Ge, M., Wu, L., Zuo, J. et al. (2013). Adsorption of heavy metal ions from aqueous solution by carboxylated cellulose nanocrystals. *Journal of Environmental Sciences, 25,* 933–943.
40. Hu, Z. H., Omer, A. M., Ouyang, X. K., Yu, D. (2018). Fabrication of carboxylated cellulose nanocrystal/sodium alginate hydrogel beads for adsorption of Pb(II) from aqueous solution. *International Journal of Biological Macromolecules, 108,* 149–157.
41. Liu, P., Borrell, P. F., Božič, M., Kokol, V., Oksman, K. et al. (2015). Nanocelluloses and their phosphorylated derivatives for selective adsorption of Ag^{+}, Cu^{2+} and Fe^{3+} from industrial effluents. *Journal of Hazardous Materials, 294,* 177–185.